CoNF-980121--

LA-UR-97-4135

Title: INVESTIGATION OF MICROPHYSICAL PARAMETERS WITHIN WINTER AND SUMMER TYPE PRECIPITATION EVENTS OVER MOUNTAINOUS TERRAIN

Author(s): JAMES R. STALKER, EES-8
JAMES E. BOSSERT, EES-8

Submitted to: AMERICAN METEOROLOGICAL SOCIETY SPECIAL SYMPOSIUM ON HYDROLOGY

PHOENIX, AZ

JANUARY 11-16, 1998

Los Alamos
NATIONAL LABORATORY

LA-UR- 97-4135

1.23 INVESTIGATION OF MICROPHYSICAL PARAMETERS WITHIN WINTER AND SUMMER TYPE PRECIPITATION EVENTS OVER COMPLEX TERRAIN

James R. Stalker + and James E. Bossert

Los Alamos National Laboratory*
Los Alamos, NM 87545

1. INTRODUCTION

Complex terrain strongly interacts with orogenic production of precipitation during both winter and summer months. Previous studies (e.g., Cotton and Anthes 1989) on terrain effects have shown that the topography plays a key role in the the amounts of precipitation through orographic lifting, topography-induced gravity wave energy interference with the ambient flow and blocking and damming of cold air (Wesley 1991). While topography plays such a role on precipitation events, precipitation processes can modify the effective influence of topography, thereby indicating a strongly coupled dynamical-microphysical system. Linearized models have shown how small hills can produce waves on the lee side of the mountain (e.g., Smith 1979). These linear models fail, however, over barriers that are high and/ or wide (> 10 km) as they introduce more nonlinearity into the mountain-induced flow. The linear analytical models are thus rendered less useful. The complexity further increases in scenarios where two mountain ranges are separated by a valley as is the case of the Rio Grande basin of northern New Mexico.

Many previous numerical studies have looked at how this nonlinearity distorts lee waves via wave breaking, cold air damming, downslope wind storms, etc. This nonlinearity changes precipitation processes which in turn change the dynamics of mountain waves (Cotton and Anthes 1989). One counter example is Cotton et al. (1986) who studied the effects of ice nucleation rates on simulated precipitation in a two dimensional numerical investigation of orographic snowfall. They found that uncertanties in the specifiaction of precipitation processes may contribute to uncertainties of 25-50% in surface precipitation amounts in stably stratified conditions.

* The Los Alamos National Laboratory is operated by the University of California for the Department of Energy (DOE).

+ *Corresponding author address:* Dr. James R. Stalker, Mail Stop D401, Los Alamos National Laboratory, Los Alamos , NM, 87545

Traditionally, in many modeling studies on orographic precipitation, the drop size distributions (DSDs) of hydrometeors are assumed to follow the well-known Marshall-Palmer (M-P) or exponential distributions. Recently, Walko et al. (1995) presented the versatility of a generalized gamma DSD on simulated total species precipitation amounts. This distribution has been incorporated into the Regional Atmospheric Modeling System (RAMS), and could be very important in realistic regional climate simulations.

In this study we investigate complex terrain effects on precipitation with RAMS for both in winter and summer cases from a microphysical perspective. We consider a two-dimensional east-west topographic cross-section in New Mexico representative of the Jemez mountains on the west and the Sangre de Cristo mountains on the east. Located between these two ranges is the Rio Grande Valley. In these two dimensional experiments, variations in DSDs are considered to simulate total precipitation that closely duplicate observed precipitation. Uncertainties of three-dimensionality and the microphysical parameterizations within RAMS may lead to discrepancies in model predicted precipitation. Future three-dimensional simulations will employ the best DSDs determined from these 2D simulations in an effort to optimize the microphysics parameterization of RAMS over the Rio Grande Basin for regional climate simulations.

2. OBSERVATIONS

Soundings used to initialize RAMS have been obtained from the station in Albuquerque, New Mexico, whose latitude, longitude and elevation are 32 N, 106 W, and 1619 m ASL respectively. The 1200 UTC 19 November 1992 sounding is used for the first winter case. The 1200 UTC 3 December sounding is used for the second winter case. The 1200 UTC 18 July 1993 is used for the summer case. Relatively weak winds (< 8 ms^{-1}) over a deep layer of 8 km MSL were observed for the first winter case. The freezing level was found near 3.25 km MSL. The freezing level for the second winter case was found near 2.8 km MSL. For the summer case there was a shallow layer of weak winds (< 3 ms^{-1}) below the freezing level of 5.0 km MSL.

Total precipitation and snow water equivalent depths from SNOTEL and CO-OP stations are used to compare total precipitation produced by the model simulations. The stations used approximately follow a transect through the topographic cross-section used in the simulations.

3. MODEL SETUP AND DESCRIPTION

3.1 Model setup

RAMS is a widely-used, comprehensive atmospheric modeling system based upon fundamental conservation relationships. A general description of RAMS can be found in Pielke et al. (1992) and many other publications. The two dimensional simulation domain has an east-west dimension of 450 km and the vertical dimension of the domain extends to ~15.0 km. The horizontal grid spacing used is 3 km while the vertical grid spacing varies from 400 m near the surface to 600 m with a stretching factor of 1.1. The time step used in these simulations is 4 s.

The model prognoses u, v, w, the ice-liquid water potential temperature (Tripoli and Cotton 1982), the perturbation Exner function, total water mixing ratio, and mixing ratios and number concentrations of all hydrometeor species. Some of the important diagnosed variables aside from the aforementioned mixing ratios are the dry air density, potential temperature, and temperature.

A rigid wall condition (w= 0.0 m s^{-1}) is used for the top boundary. The bottom boundary condition is a rigid wall (i.e., w= 0.0 m s^{-1}) with frictional effects included, i.e., no slip at the bottom boundary indicating the fact that the horizontal velocities go to zero as well. The thermodynamic variables at the bottom boundary are extrapolated linearly from the prognosed values at two grid points above the boundary (Knupp 1985). The current study employs the Klemp-Lilly type lateral boundary condition.

A surface layer scheme based on a soil model developed by Tremback and Kessler (1985) is used in this study. This scheme also includes a vegetation model based on Avissar and Pielke (1989) that has 18 different types of vegetation. We have used the radiation scheme of Mahrer and Pielke (1977) in the current study. A modified Kuo-type cumulus parameterization scheme is also included.

A first-order turbulence clousure scheme is used in horizontal diffusion computations. A Mellor and Yamada (1974) scheme is used to descirbe vertical diffusion which is based on a second-order turbulent kinetic energy (TKE) formulation, in which the TKE is prognosed by solving the Reynolds stress term with an isotropic turbulence assumption.

3.2 Microphysics description

The current study uses RAMS version 3b which has a partial two moment microphysics scheme (Walko et al. 1995) in that the pristine ice crystal concentration and mixing ratio are fully prognosed while only one of the two quantities (i.e., either the mixing ratio or the number concentration) of the remaining categories (except cloud water) can be prognosed. Water can exist in eight different forms: 1) water vapor, 2) cloud water, 3) rain water, 4) pristine ice crystals, 5) snow, 6) graupel, 7) aggregates and 8) hail. The last seven are the actual hydrometeor types and vapor is included for completeness. The cloud water mixing ratio is diagnosed from prescribed number concentration known as the cloud condensation nuclei (CCN). We used a value of 300 for the CCN. Future two dimensional simulatations will include variations in CCN and the resulting differences in simulated precipitation amounts. Cloud water and pristine ice crystals nucleate by vapor diffusion. Once nucleated they can further grow through diffusion. Cloud water can also grow by autoconversion. This is a process by which rain drops initially form. Once rain drops form they can further grow by vapor diffusion but more importantly through a process called collision-coalescence, in which the rain drops collect cloud droplets and other rain drops to grow larger.

Pristine ice crystals, snow and aggregates are assumed to be completely frozen. Graupel and hail are the mixed phase hydrometeors which can have liquid water in them. Pristine crystals are allowed to grow by vapor diffusion only. Large pristine crystals with diameters, $\geq$ 125.0 μm, are categorized as snow indicating a bimodal distribution of pristine crystal sizes. Aggregates are formed by collision and coalescence of pristine crystals, snow, and/or other aggregates. Pristine crystals, snow and aggregates are considered low density ice.

Graupel is a mixed phase hydrometeor with a prescribed percent of liquid water (30.0 % is used in the current study) that forms through moderate to heavy riming. The other mixed phase hydrometeor is hail which can form from frozen cloud droplets and smaller rain drops and/or riming or melting of graupel. Hail is allowed to retain liquid water to as much as 99.0% but not 100.0% in which case it is recategorized as rain. In this formulation, hail can form from melting snowflakes or aggregates.

All the seven types of hydrometeors follow a generalized gamma size distribution as described by Flatau et al. (1989) and Verlinde et al. (1990). This distribution function is expressed as,

$$f_{gam}(D) = \frac{1}{\Gamma(\nu)}(\frac{D}{D_n})^{\nu-1}\frac{1}{D_n}\exp[-\frac{D}{D_n}] \quad (1)$$

where D ($0.0 \leq D \leq \infty$) is the diameter of the hydrometeor.

$\Gamma(\nu)$ is a normalization constant used in $\int_0^\infty f_{gam}\, dD = 1.0$.

D_n and ν are the characteristic diameter and a shape parameter respectively.

For $\nu = 1.0$, the gamma distribution assumes M-P distribution. As ν increases the peak value of the gamma distribution moves to the right indicating the fact that the distribution peaks at larger diameters and at the same time the distribution becomes narrower.

The third moment of the gamma distribution gives a measure of the mass (or mixing ratio) of a hydrometeor while the first moment gives the mean diameter of the distribution. By defining power laws for mass and terminal velocity as a function of diameter D one can relate the hydrometeor mixing ratio in terms of the characteristic diameter (D_n), total number concentration (N_t), α_m, β_m, and ν as

$$r = \frac{N_t}{\rho_a}\alpha_m {D_n}^{\beta_m}\frac{\Gamma(\nu+\beta_m)}{\Gamma(\nu)} \quad (2)$$

where r is the mixing ration of the hydrometeor, ρ_a is the air density.

It is seen from equation 2 that there are three free parameters (r, N_t and D_n) once the power law constants are provided by the modeler.

In the single moment formulation, where only mixing ratios of hydrometeors are prognosed (with the exception of pristine crystals), either a user specified total number concentration or a mean diameter $D_{\overline{m}}$ is needed to determine the other from 4.5. However, the modeler has to provide the values of α_m, β_m, α_{vt}, β_{vt}, and ν for each hydrometeor type.

The mean diameter $D_{\overline{m}}$ of a hydrometeor is related to the characteristic diameter D_n and ν as shown by,

$$D_{\overline{m}} = D_n(\frac{\Gamma(\nu+\beta_m)}{\Gamma(\nu)})^{\frac{1}{\beta_m}} \quad (3)$$

where $D_{\overline{m}}$ is the mean diameter of the hydrometeor size distribution.

In version 3b, both homogeneous and heterogeneous types of ice nucleation are allowed. In heterogeneous nucleation an ice nucleus (IN) leads to an ice crystal either from vapor deposition or freezing of water. The ambient temperature required for homogeneous nucleation to occur is below -40.0 ^{0}C.

Deposition nucleation and contract-freezing nucleation are combined to give an ice crystal concentration given by (4) (Meyers et al 1992).

$$(N_t)_d = exp(6.269 + 12.96 r_{si}) \quad (4)$$

where r_{si} is the saturation pressure over ice.

Deposition nucleation occurs when vapor comes in contact with an IN. This is supposed to occur when supersaturations of r_{si} are achieved and the ambient temperature is below -5.0 ^{0}C. Condensation-freezing occurs when an IN also exhibits the property of a CCN. Vapor condenses onto the IN because of its CCN property and will eventually freeze. This type of nucleation occurs when the ambient temperature is below -2.0 ^{0}C.

Contact freezing takes place as supercooled water may come in contact with an IN leading to instant freezing. There are three processes by which such an IN can be brought close to supercooled water: 1) diffusiophoresis, 2) thermophoresis, and 3) Brownian motion. The above three processes are parameterized as given by (5) (Meyers et al. 1992).

$$N_a = \exp(4.11 - 0.262 T_{cc}) \quad (5)$$

where T_{cc} is the cloud droplet temperature.

DeMott et al. (1994) derived formulas for homogeneous nucleation of supercooled water and nucleation from unactivated haze particles. The reader is referred to DeMott et al. (1994) for their empirical formulations. It is important to note that the homogeneous nucleation of supercooled water is primarily a function of temperature but impurities within the supercooled water affect the actual nucleation rates. The nucleation due to unactivated haze particles is affected by temperature, humidity, curvature, etc.

4. RESULTS

Results of two-dimensional idealized simulations for two winter cases and one summer case are presented in this paper. The first winter case is a less severe winter precipitation event that occurred during the latter half of November 1992 while the second winter storm occurred during the first half of December 1992. The summer precipitation event occurred in the latter half of July 1993.

Based on these simulations, we have identified two mechanisms that are important in producing the differences in simulated total precipitation for both winter and summer events. The first mechanism by which relative effectiveness of vapor depletion either to cloud water or pristine crystals is created. This mechanism is relevant in winter storms only. The second mechanism is also related to effectiveness of vapor depletion but this depletion is to rain water through increased autoconversion and not to pristine crystals and/ or snow. This mechanism is, thus, relevant in summer precipitation events only. These two mechanisms are illustrated using different cases in terms of simulated accumulated precipitation amounts in the following separate sections.

4.1 Winter cases

In simulating winter precipitation events, one can change the relative effectiveness of vapor depletion by cloud water or pristine crystals by changing the shape parameter. Larger values for the shape parameter lead to smaller number of larger cloud particles and thus reduction in effective surface area of cloud droplets to diffuse vapor. This leads to relatively lesser amounts of cloud water and increased amounts of pristine crystals and/ or snow. These increased amounts of pristine crystals and/ or snow then lead to increased amounts of aggregates and reduced amounts of graupel (see section 4.1.1). If the reductions in cloud water upon increased values for the shape parameter is not significant, for example, when the supersaturations are relatively strong indicating significant updrafts, increased amounts of pristine crystals and/ or snow are produced but at the same time pronounced reductions in graupel amounts may not necessarily occur as some aggregates get rimed to become graupel (see section 4.1.2).

4.1.1 Case 1: 19 November 1992

This case produced the lowest precipitation of all simulations for the M-P DSDs. The total amount of precipitation accumulated over a 24-hour period is ~ 0.2 mm (see Fig. 1). The dominant type of hydrometeor is aggregates whose total accumulations are ~ 0.2 mm.

For a shape parameter of 1.5, the total precipitation as well as aggregates have increased to ~ 0.35 mm (Fig. 2). The dominant type of hydrometeor, again, is aggregates. The main difference in the two runs, however, is that accumulation of graupel is reduced from ~ 0.1 mm (see Fig. 1) to ~ 0.05 mm (see Fig. 2). This is a result of the first mechanism discussed in this paper.

4.1.2 Case 2: 3 December 1992

The total precipitation, aggregate and graupel amounts are 23 mm, 9 mm, and 14 mm respectively with the M-P DSDs (see Fig. 3). For a shape of 1.5, the total precipitation has increased from 23 mm to 25 mm and at the same time, the amount of aggregates has increased too from 9 mm (see Fig. 3) to ~ 13 mm (see Fig. 4). However, the amount

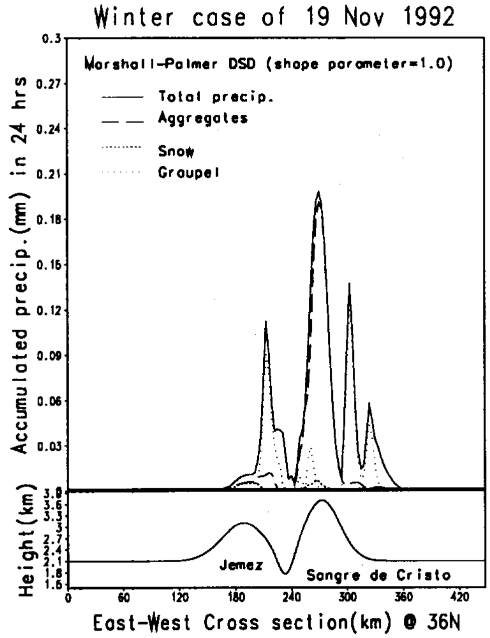

Figure 1. Accumulated total, aggregates, snow and graupel precipitation amounts (mm) of water equivalent depth for 19 November 1992 case (with the M-P DSDs).

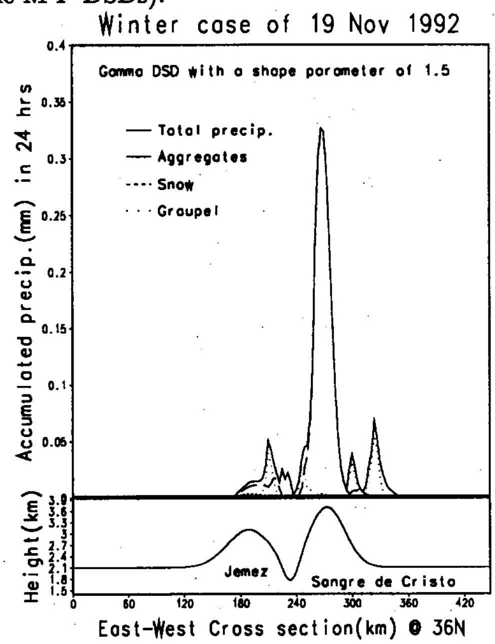

Figure 2. Accumulated total, aggregates, snow and graupel precipitation amounts (mm) of water equivalent depth for 19 November 1992 case (with a shape parameter of 1.5).

of graupel in these two runs has changed negligibly.

It is obvious from the two winter cases analyzed in this study that the amount of graupel may or may not decrease by increasing the shape parameter. We offer two reasons why corresponding reductions in graupel amounts are not simulated with larger values for the shape parameter as expected. Firstly, reduction of cloud water due to increased shape parameter may not be pronounced so riming is totally elimininated, i.e., graupel can still exist. Secondly, increased aggregation will also lead to production of graupel due to riming of aggregates for these conditions. This is illustrated in the second winter case (see Fig. 4).

4.2 Summer case

As mentioned earlier, the second mechanism is crucial in summer events. Larger values for the shape parameter lead to larger cloud particle mean diameters. Autoconversion rate of cloud water to rain water through continued condensation increases as the mean diameter of cloud DSD increases (Berry and Reinhardt 1974). This increased rate of autoconversion produces more rain and thus more hail (see section 4.2.1).

4.2.1 Case 1: 18 July 1993

For the M-P DSDs, the simulated total precipitation is ~ 5.5 mm (Fig. 5). This precipitation is mostly in the form of hail. Very little amount of rain (only ~ 0.018 mm) is produced in this simulation. The total simulated precipitation is increased further by increasing the shape parameter from 1.0 to 1.5. The total simulated precipitation for this case is ~ 9 mm (see Fig. 6). Again this precipitation is mostly in the form of hail with negligible amount of rain (~ 0.055 mm).

The summer case simulations show that increased autoconconversion due to larger values for the shape parameter lead to more rain and hail. These negligible amounts of rain and very large amounts of hail are a consequence of how hail is parameterizations in the model. There are, at least, two reasons for this relatively larger amounts of hail compred to rain: 1) the percentage of liquid water retained in hail is 99% (section 3 for details), 2) the mean diameter of hail is 3 mm compared to 1 mm for rain.

5. CONCLUSIONS AND FUTURE WORK

Variations in DSDs used in the two dimensional experiments produce significant differences in total accumulated precipitation amounts and the types of precipitatoin. These two-dimensional idealized simulations suggest that DSDs with a shape parameter of 1.5 produce accumulated precipitation close to the observed precipitation amounts than the M-P distributions.

Future work will involve more two-dimensional simulations with increased values for the shape parameter and variations in species mean diameters as well.

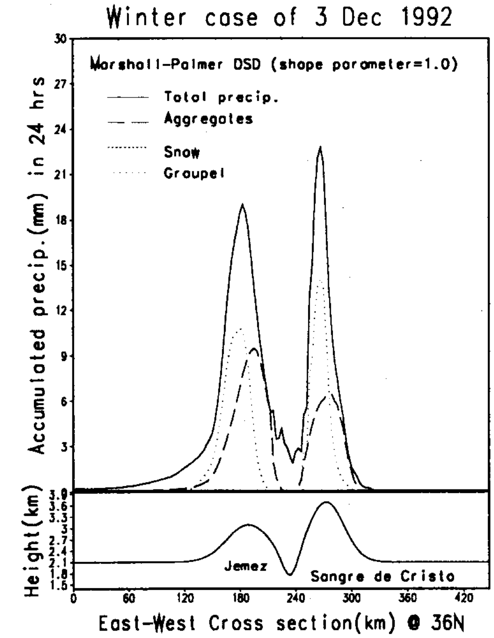

Figure 3. Accumulated total, aggregates, snow and graupel precipitation amounts (mm) of water equivalent depth for 3 December 1992 case (with the M-P DSDs).

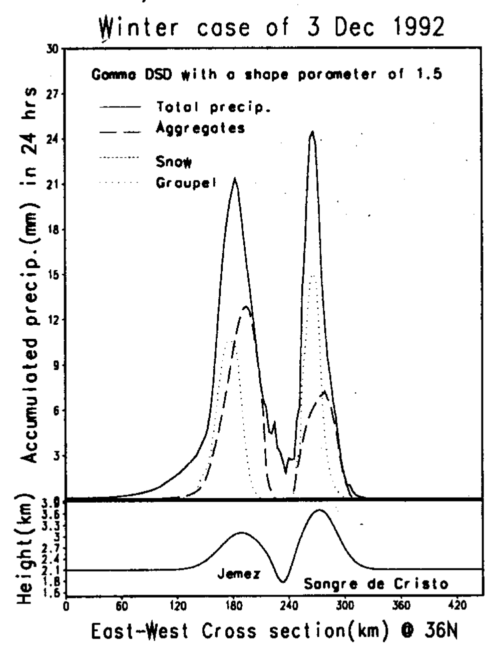

Figure 4. Accumulated total, aggregates, snow and graupel precipitation amounts (mm) of water equivalent depth for 3 December 1992 case (with a shape parameter of 1.5).

ACKNOWLEDGEMENTS

We acknowledge Mr. David L. Langley's help with the SNOWTEL/ CO-OP data sets. Discussions with Dr. Jon M. Reisner, Dr. Keeley

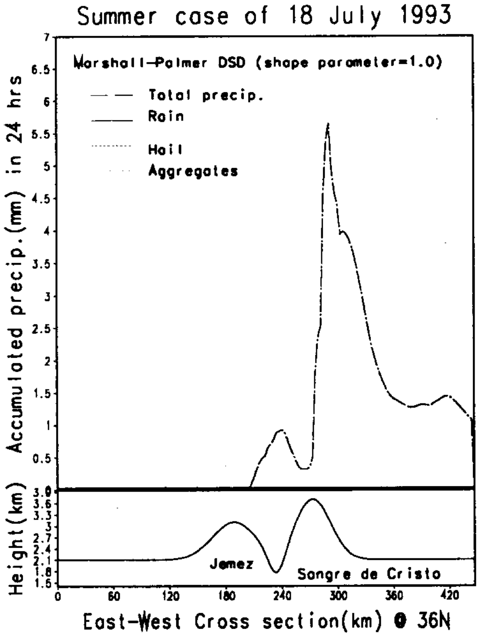

Figure 5. Accumulated total, rain, hail, and aggregate precipitation amounts (mm) for 18 July 1993 case (with the M-P DSDs).

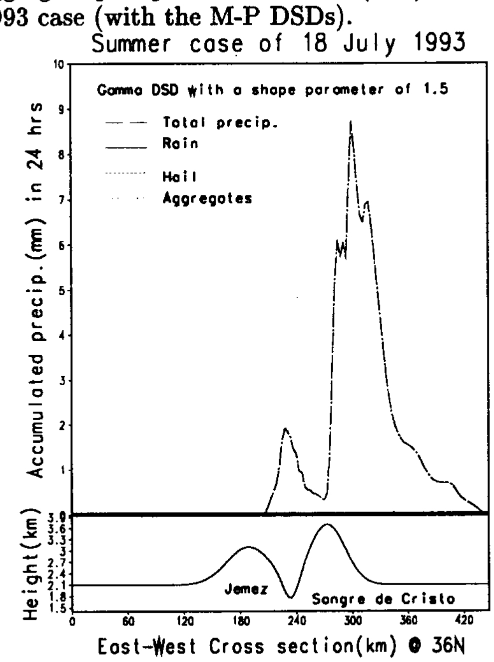

Figure 6. Accumulated total, rain, hail, and aggregate precipitation amounts (mm) for 18 July 1993 case (with a shape parameter of 1.5).

R. Costigan, and Dr. J. T. Lee have been very valuable during this study.

REFERENCES

Avissar and Pielke 1989: A parameterization of heterogeneous land surfaces for atmospheric numerical mod els and its impact on regional meteorolgy. *Mon. Wea. Rev.*, **117**, 2113-2136.

Cotton and Anthes 1989: Storm and cloud dynamics, Academic Press, *International Geophysics Series*, vol. **44**.

Cotton et al. 1986: Numerical simulation of the effects of varying ice crystal nucleation rates and aggregation processes on orographic snowfall. *J. Climate Appl. Meteorol.*, **25**, 1658-1680.

DeMott et al. 1994: Parameterization and impact of ice initiation processes relevant to numerical model simulations of cirrus clouds. *J. Atmos. Sci.*, **51**, 77-90.

Flatau et al. 1989: The CSU-RAMS cloud microphysical module: General theory and code documentation. Paper no. 451, Dept. Atmos. Sci., Colorado State Univ., Fort Collins, CO.

Knupp 1985: Precipitating convective downdraft structure: A synthesis of observations and modeling. Ph. D. Thesis, Dept. Atmos. Sci., Colorado State Univ., Fort Collins, CO.

Mahrer and Pielke 1977: A numerical study of the airflow over irregular terrain. *Beitrage zur Phys der Atmosphare*, **50**, 98-113.

Mellor and Yamada 1974: A hierarchy of turbulence closure models for planetary boundary layers. *J. Atmos. Sci.*, **31**, , 1791-1806.

Meyers et al. 1992: New primary ice nucleation parameterizations in an explicit cloud model. *J. App l. Meteor.*, **31**, 708-721.

Pielke et al. 1992: A comprehensive meteorological modeling system-RAMS. *Meteor. and Atmos. Phys.*, **49**, 69-91.

Smith 1979: The influence of mountains on the atmosphere. *Adv. Geophysics*, **21**, 87-230.

Tremback and Kessler 1985: A surface temperature and moisture parameterization for use in mesoscale nume rical models. *Pr eprints, 7th Conf. on Numerical Wea. Prediction*, 17-20 June 1985, Montreal, Canada, AMS.

Tripoli and Cotton 1982: A numerical investigation of several factors leading to the observed variable i ntensity of deep conv ection over south Florida. *J. Appl. Meteor.*, **19**, 1037-1067.

Verlinde et al. 1990: Analytical solutions to the collection growth equation: Comparison with approximate methods and applicat ion to cloud microphysics parameterization schemes. *J. Atmos. Sci.*, **47**, 2871-2880.

Walko et al. 1985: The regional atmospheric modeling system (RAMS): User's guide (version 3b).

Wesley 1991: An investigation of the effects of topography on Colorado front range winter storms, M.S. Thesis, paper no. 489, Dept. Atmos. Sci., Colorado State Univ., Fort Collins, CO.

M98003012

Report Number (14) LA-UR--97-4135
CONF-980121--

Publ. Date (11) 199710
Sponsor Code (18) DOE/MA, XF
UC Category (19) UC-902, DOE/ER

DOE